Engineering Reports

WILEY

Engineering Reports Open Access

RESEARCH ARTICLE OPEN ACCESS

Existence, Stability, and Data-Driven Analysis of a Fractional-Order Avian Influenza Model in Poultry Farms

Muhammad Altaf Khan[1,2,3,4] | Mahmoud H. DarAssi[5] | Irfan Ahmad[6] | Ebraheem Alzahrani[7] | Nurulfiza Mat Isa[1]

[1]Laboratory of Vaccine and Biomolecules, Institute of Bioscience, Universiti Putra Malaysia, Serdang, Malaysia | [2]School of Health and Environmental Science, Korea University, Seoul, South Korea | [3]Faculty of Natural and Agricultural Sciences, University of the Free State, Bloemfontein, South Africa | [4]Department of Mathematics, Saveetha School of Engineering, SIMATS, Saveetha University, Chennai, India | [5]Department of Basic Sciences, Princess Sumaya University for Technology, Amman, Jordan | [6]Department of Clinical Laboratory Sciences, College of Applied Medical Science, King Khalid University, Abha, Saudi Arabia | [7]Department of Mathematics, Faculty of Science, King Abdulaziz University, Jeddah, Saudi Arabia

Correspondence: Muhammad Altaf Khan (altafkhan@upm.edu.my; muhammadaltafkhan@korea.ac.kr; altafdir@gmail.com)

Received: 17 January 2026 | **Revised:** 24 February 2026 | **Accepted:** 6 March 2026

Keywords: chicken disease influenza model | fractional order model | numerical results | stability analysis

ABSTRACT

In the present analysis, we consider a chicken disease model in fractional derivatives. The fractional model and its related results are discussed. We present the solution's existence and its uniqueness for the fractional chicken model. Stability at the Disease-free equilibrium is shown, and found that when $\mathcal{R}_0 < 1$, the model is locally asymptotically stable. The existence of an endemic equilibrium when $\mathcal{R}_0 > 1$ shows a unique endemic equilibrium. A numerical scheme to get the solution for the fractional chicken model is presented. Based on the real farm data in Bangladesh, the model is fitted, and the respective values of the parameters are obtained. We present graphical results to show that the disease can be eliminated under various conditions on model parameters. Using real farm data and an 80% vaccine efficacy, we show that the treatment, together with vaccine efficacy, makes the disease controllable.

1 | Introduction

Avian influenza (AI) is a contagious viral disease that mostly infect birds species but sometimes also infects humans. It was reported in East China [1]. The infection spreads largely through the migratory birds, while local wild birds contribute to the transmission of the disease within their natural habitats [2]. Furthermore, local chickens may become infected by ingesting feces contaminated with the virus, and make the disease spreadable through the oral-fecal route [3]. LPAI (low pathogenic) and HPAI (highly pathogenic) are the two subtypes of AI. Sometimes, under certain conditions in chickens, LPAI viruses can replicate extensively, leading to increased pathogenicity [4]. HPAI viruses usually cause severe illness and high death rates in chickens [2], while LPAI causes moderate clinical symptoms, significantly reduces egg production, but only slightly increases mortality [5]. After developing a dynamic model based on real data, the authors in [6] found that seasonal temperature variations significantly affect avian influenza transmission. Seasonality is a major factor in the spread of AI in chicken, and the migration of wild birds contributes to these seasonal changes [2]. Using real data gathered over time from infected farms, a mathematical model captures the seasonal patterns of AI, showing yearly, semi-yearly, or both of them [2, 7]. Based on the yearly peak in their 12-month data, the researchers in [7] summarized that AI dynamics under annual seasonality pose a notable risk of spilling over to other species. To identify the high-risk periods, the authors in [2] analyzed the seasonal pattern of AI. A significant seasonal risk occurs over four months was found around four months (November to February), peaking in January.

Classical epidemic models, such as SIR and SEIR, predict constant, steady-state epidemics when permanent immunity is assumed. The AI in humans and birds' dynamics through a mathematical model was considered in the study [8], and also established results for their steady-state epidemic. To examine the impact of vaccination and environmental viruses on chickens, the authors in [9] formulated an avian influenza transmission model. Additionally, they showed that immunization of chickens can significantly reduce human infections and that the risk of infection is higher in colder climates. To understand the avian influenza, the work in [10] strongly advocated an ecological model and demonstrated the necessity of including nonlinear relationships among infected and vulnerable population sizes. Additionally, they demonstrated how different chicken epidemics had different zoonotic transmission components, which were identified as the primary cause of H5N1 spillover transmission in Bangladesh. Due to high mortality rates, the authors in [11] used an SEIR-type model to estimate farm-specific transmission rates and describe the within-flock dynamics of highly pathogenic AI. The researchers in [12] defined several fundamental characteristics using the basic reproduction number and proposed a reaction-diffusion model with periodicity in time to represent AI infection among humans and poultry. Nonetheless, the seasonal effects of viral infection have been observed by many researchers in their models [8–13].

Long-term health risks in humans and natural systems can be predicted by seasonality [14]. It also influences host-pathogen dynamics and vector behavior [15]. Epidemic, biennial cycles, and even chaotic dynamics may be induced by seasonal forcing [16–19]. Numerous researchers have examined the nonlinear impact of periodically changing contact rates in epidemic models [15, 20]. Among these studies, the authors in [15] explained the way in which seasonality can affect the disease spread. The authors in [18] showed that periodic variation in contact rates over a single year in the classic epidemic models, such as SIR and SEIR types, can induce solutions with periods longer than one year. Authors in [16] showed that the epidemic models with small periodic fluctuations can go through a series of period-doubling bifurcations. In [13], the authors formulated a compartmental model to explain the spread of AI in chicken farms, but classical epidemic models are unable to explain the recurrent outbreaks [16, 21]. There is no approved antiviral that exists [22], oseltamivir, and chicken interferon-alpha show potential in reducing avian influenza virus replication and shedding in poultry [23–26].

Mathematical models constructed using fractional derivatives are of great importance; among their key features are heredity properties, memory effects, and crossover behavior, etc. It has been shown that the order of the fractional derivative helps models better fit real data, due to the flexibility offered by fractional orders, whereas integer-order models lack such flexibility. In disease epidemiology and other scientific fields, extensive research has employed fractional-order derivatives, see [27–36]. For example, Zika virus model with mutation using non-integer order derivatives was considered in [27]. The Caputo–Fabrizio fractional derivative was applied to model COVID-19 transmission in [28]. In [29], the authors investigated coffee berry disease using a fractional approach. An infectious disease model incorporating social media effects was studied in [30]. In [31], an infectious disease model with optimal control and cost-effective analysis was formulated using fractional-order derivatives. A fractional-order model was used to analyze the flow dynamics of financial markets in [32]. The fractional modeling approach for bone dynamics was proposed in [33]. In [34], the authors analyzed a fractional-order Hepatitis B model incorporating socio-economic factors. An influenza model formulated with fractional derivatives, including control strategies and stability analysis, was presented in [35]. Finally, the dynamics of gambling behavior were modeled using fractional derivatives in [36]. In [37], a fractional model is proposed to investigate COVID-19 in Italy, while in [38] an SEIR fractal-fractional order model is proposed to investigate COVID-19 infection dynamics. Similarly, the fractional model is proposed to study diabetes in [39], the fractional monkeypox model [40], and to study the stability of a fractional system is given in [41].

In the present study, we formulate an influenza model for chicken disease using reported case data. We establish the model and discuss its mathematical properties. The positivity, boundedness, and uniqueness of solutions of the fractional system are presented. Equilibria are obtained, and their stability results are evaluated. A numerical scheme and its results based on real data are obtained and discussed. Various results regarding disease elimination are demonstrated. The section-wise structure of the paper is as follows: Section 2 discusses the model constructions of an influenza chicken disease in integer and non-integer order derivatives. The analysis of the chicken influenza model is presented in Section 3. In Section 4, the equilibria and their analysis are discussed. The numerical approach and discussion of results are presented in Section 5. Section 6 summarizes the findings of the study and presents the concluding remarks.

2 | Model Construction

Here, we construct a mathematical model for the transmission of seasonal avian influenza (chicken) incorporating seasonal effects. The total chicken population is divided into six compartments: Susceptible $S(t)$, exposed $E(t)$, symptomatic infected $I_s(t)$, asymptomatic infected $I_a(t)$, treated $T(t)$, and recovered $R(t)$. The total population at time t, denoted by $N(t)$, is given by $N(t) = S(t) + E(t) + I_s(t) + I_a(t) + T(t) + R(t)$. The model that governs the system of nonlinear differential equations is given by:

$$\begin{cases} \dfrac{dS(t)}{dt} = \Lambda - \tau\Phi S(t) - (1-\tau)S(t) - dS(t), \\ \dfrac{dE(t)}{dt} = \tau\Phi S(t) - \delta E(t) - dE(t), \\ \dfrac{dI_s(t)}{dt} = \theta\delta E(t) - (\phi_1 + \psi_1 + \alpha_1 + d)I_s(t), \\ \dfrac{dI_a(t)}{dt} = (1-\theta)\delta E(t) - (\phi_2 + \psi_2 + \alpha_2 + d)I_a(t), \\ \dfrac{dT(t)}{dt} = \phi_1 I_s(t) + \phi_2 I_a(t) - (\psi_3 + \alpha_3 + d)T(t), \\ \dfrac{dR(t)}{dt} = \psi_1 I_s(t) + \psi_2 I_a(t) + \psi_3 T(t) \\ \qquad\qquad + (1-\tau)S(t) - (\alpha_4 + d)R(t), \end{cases} \tag{1}$$

where

$$\Phi = \frac{\eta(t)(I_s(t) + \kappa_1 I_a(t) + \kappa_2 T(t))}{N(t)}.$$

The contact rate $\eta(t)$ is assumed to be continuous, positive, periodic function with a 12-month cycle. It can be modeled in the following form:

$$\eta(t) = \eta_0\left(1 + \eta_1\left(\cos\left(\frac{2\pi t}{12} + \nu\right)\right)\right), \tag{2}$$

where η_0 represents the baseline contact rate, η_1 is the amplitude of seasonal variation ($0 \le \eta_1 \le 1$), while ν is the phase shift. The model is subjected to the initial conditions (ICs) given by:

$$\begin{aligned} &S(0) = S_0 > 0,\ E(0) = E_0 \ge 0,\ I_s(0) = I_{s0} \ge 0,\\ &I_a(0) = I_a 0 \ge 0,\ T(0) = T_0 \ge 0,\ R(0) = R_0 \ge 0. \end{aligned} \tag{3}$$

The farmers provide vaccines to all chickens in the farms, but still, vaccine failure occurs because no vaccine is perfect. Considering vaccine inefficacy by τ, then $\tau S(t)$ chickens will be sick through the infection while the rest get permanent immunity at the rate $(1-\tau)S(t)$. The natural death rate is d while the birth rate is Λ. The contact rate for the disease transmission is given by $\eta(t)$. A portion of individuals become symptomatic infected at the rate $\theta\delta$, while remaining $(1-\theta)\delta$, where δ is the incubation period. The parameters κ_1 and κ_2 are the relative transmission rates for symptomatic and asymptomatic individuals. The treatment rates for symptomatic and asymptomatic individuals are denoted by ϕ_1 and ϕ_2, respectively. The recovery rates ψ_1, ψ_2, and ψ_3, respectively, represents for the symptomatic, asymptomatic, and treated individuals. α_1, α_2, α_3, and α_4 are the induced death rates associated with the symptomatic, asymptomatic, treated, and recovered individuals, respectively.

2.1 | Fractional Model

Fractional order models are more appropriate than the classical order. One of the reasons is the involvement of crossover behavior, heredity properties, application to real data fittings, and the memory effects. Based on these properties, we generalize system (1) to a fractional-order model using the Caputo derivative, and present the following system:

$$\begin{cases} D_t^\alpha S = \Lambda - \tau\Phi S(t) - (1-\tau)S(t) - dS(t),\\ D_t^\alpha E = \tau\Phi S(t) - \delta E(t) - dE(t),\\ D_t^\alpha I_s = \theta\delta E(t) - (\phi_1 + \psi_1 + \alpha_1 + d)I_s(t),\\ D_t^\alpha I_a = (1-\theta)\delta E(t) - (\phi_2 + \psi_2 + \alpha_2 + d)I_a(t),\\ D_t^\alpha T = \phi_1 I_s(t) + \phi_2 I_a(t) - (\psi_3 + \alpha_3 + d)T(t),\\ D_t^\alpha R = \psi_1 I_s(t) + \psi_2 I_a(t) + \psi_3 T(t)\\ \qquad + (1-\tau)S(t) - (\alpha_4 + d)R(t), \end{cases} \tag{4}$$

where $\alpha \in (0,1]$ is the fractional order in the Caputo sense, and D_t^α represents the fractional derivative [42, 43]. Let $m = \lceil \alpha \rceil$ be the smallest integer greater than or equal to α. For a function $y(t)$, the Caputo derivative of order α is defined as follows:

$$D^\alpha y(t) = \frac{1}{\Gamma(m-\alpha)}\int_0^t (t-\gamma)^{m-\alpha-1} y^{(m)}(\gamma)d\gamma, \quad t > 0, \tag{5}$$

where $\alpha \in (m-1, m]$. Accordingly, for a function $y(t)$, the fractional integral in the Riemann–Liouville sense is defined as follows:

$$I^\alpha y(t) = \frac{1}{\Gamma(\alpha)}\int_0^t (t-\gamma)^{\alpha-1} y(\gamma)d\gamma. \tag{6}$$

The complete transmission diagram of the model (1) is shown in Figure 1.

3 | Model Analysis

In the present section, we present the fundamental results associated with the fractional influenza chicken disease model (4). We show first the non-negativity of the model.

Theorem 1. *Every solution of the fractional-order influenza model (4) is uniformly bounded and non-negative.*

Proof. By using model (4), the following is obtained:

$$\begin{aligned} D_t^\alpha\Big|_{S=0} &= \Lambda \ge 0,\\ D_t^\alpha\Big|_{E=0} &= \frac{\eta(t)(I_s + \kappa_1 I_a + \kappa_2 T)}{N - E} \ge 0,\\ D_t^\alpha\Big|_{I_s=0} &= \theta\delta E \ge 0,\\ D_t^\alpha\Big|_{I_a=0} &= (1-\theta)\delta E \ge 0,\\ D_t^\alpha\Big|_{T=0} &= \phi_1 I_s + \phi_2 I_a \ge 0,\\ D_t^\alpha\Big|_{R=0} &= \psi_1 I_s + \psi_2 I_a + \psi_3 T \ge 0. \end{aligned} \tag{7}$$

According to the findings in [44], the solution is therefore still in $\mathcal{R}_+^6$. Moreover, summing the model Equations (4), and using $N = S + E + I_s + I_a + T + R$, we obtain

$$\begin{aligned} D_t^\alpha N &= \Lambda - dN - \alpha_1 I_s - \alpha_2 I_a - \alpha_3 T - \alpha_4 R,\\ &\le \Lambda - dN. \end{aligned} \tag{8}$$

We arrive at the following result by using [45],

$$N(t) \le \frac{\Lambda}{d} + \left(N(0) - \frac{\Lambda}{d}\right)E_\alpha(-dt^\alpha), \tag{9}$$

where E_α is the Mittag–Leffler function. Therefore, $N(t) \to \Lambda/d$ when $t \to \infty$, and $0 < N(t) \le \Lambda/d$. As a result, all solutions beginning in $\mathcal{R}_+^6$ are limited to the region Ω, where

$$\Omega = \left\{(S, E, I_s, I_a, T, R) | 0 \le N \le \frac{\Lambda}{d}\right\}. \tag{10}$$

□

We now show that the solution associated with the influenza model (4) exists and is unique. We provide the following result:

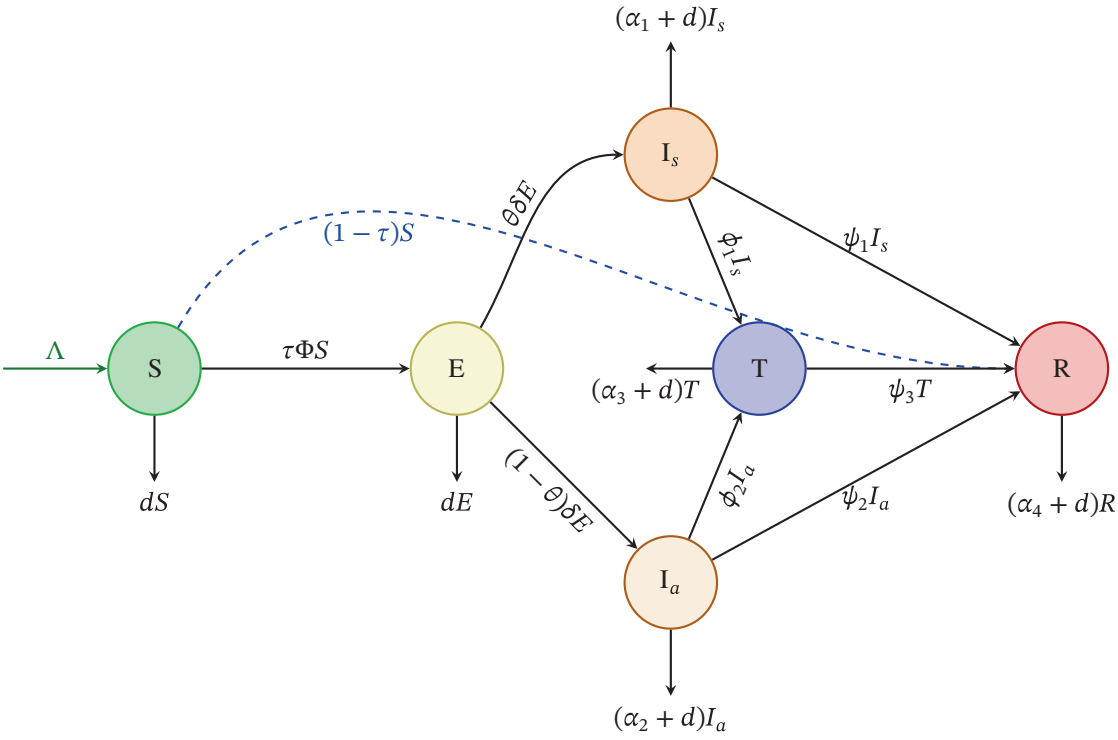

FIGURE 1 | The flowchart represents the transmission diagram of the fractional chicken influenza model (1), where the circles are the compartments and the arrows indicate the transfer rate.

Theorem 2. *The influenza fractional chicken disease model (4) possesses a unique solution.*

Proof. Let $Y(t) = (S, E, I_s, I_a, T, R)^{Tra} = (y_1, y_2, y_3, y_4, y_5, y_6)^{Tra}$, where Tra denotes the transpose. Then, we can express system (4) in the following form:

$$D_t^{\alpha} Y(t) = \mathcal{Y}_1 Y(t) + F(t, Y) + \mathcal{Y}_3, \tag{11}$$

where the matrices $\mathcal{Y}_1$, $F(t, Y)$, and $\mathcal{Y}_3$ are defined as:

$$\mathcal{Y}_3 = \begin{pmatrix} \Lambda \\ 0 \\ 0 \\ 0 \\ 0 \\ 0 \end{pmatrix}.$$

$$\mathcal{Y}_1 = \begin{pmatrix} -(1-\tau) - d & 0 & 0 & 0 & 0 & 0 \\ 0 & -(\delta + d) & 0 & 0 & 0 & 0 \\ 0 & \theta\delta & -(\phi_1 + d + \alpha_1 + \psi_1) & 0 & 0 & 0 \\ 0 & (1-\theta)\delta & 0 & -(\phi_2 + d + \alpha_2 + \psi_2) & 0 & 0 \\ 0 & 0 & \phi_1 & \phi_2 & -(\psi_3 + d + \alpha_3) & 0 \\ (1-\tau) & 0 & \psi_1 & \psi_2 & \psi_3 & -(d + \alpha_4) \end{pmatrix},$$

$$F(t, Y) = \begin{pmatrix} -\tau\Phi S & 0 & 0 & 0 & 0 & 0 \\ \tau\Phi S & 0 & 0 & 0 & 0 & 0 \\ 0 & 0 & 0 & 0 & 0 & 0 \\ 0 & 0 & 0 & 0 & 0 & 0 \\ 0 & 0 & 0 & 0 & 0 & 0 \\ 0 & 0 & 0 & 0 & 0 & 0 \end{pmatrix},$$

Consider $G(t, Y(t)) = \mathcal{Y}_1 Y(t) + F(t, Y) + \mathcal{Y}_3$. We aim to verify that $G(t, Y(t))$ fulfills the Lipschitz condition:

$$\begin{aligned} \|G(t, Y(t)) - G(t, \overline{Y}(t))\| &= \|\mathcal{Y}_1 Y(t) + F(t, Y) + \mathcal{Y}_3 \\ &\quad - (\mathcal{Y}_1 \overline{Y}(t) + F(t, \overline{Y}) + \mathcal{Y}_3)\|, \\ &= \|\mathcal{Y}_1 (Y(t) - \overline{Y}(t)) + F(t, Y) - F(t, \overline{Y})\|. \end{aligned}$$

By the triangle inequality and properties of induced matrix norms, we obtain

$$\begin{aligned}\|G(t,Y(t))-G(t,\overline{Y}(t))\|&\leq \|\mathcal{Y}_1(Y(t)-\overline{Y}(t))\|+\|F(t,Y)-F(t,\overline{Y})\|,\\&\leq \|\mathcal{Y}_1\|\ \|Y(t)-\overline{Y}(t)\|+\|F(t,Y)-F(t,\overline{Y})\|.\end{aligned}$$

Since $\|\mathcal{Y}_1\|$ denotes the induced norm of the constant matrix $\mathcal{Y}_1$, let

$$L_1=\|\mathcal{Y}_1\|.$$

The nonlinear part $F(t,Y)$ involves the term

$$\Phi(t,Y)=\frac{\eta(t)(I_s+\kappa_1 I_a+\kappa_2 T)}{N},$$

which is linear in Y and, on any region where the total population $N(t)$ is bounded away from zero, satisfies a Lipschitz bound

$$\|F(t,Y)-F(t,\overline{Y})\|\leq L_2\ \|Y-\overline{Y}\|$$

for some constant L_2. Thus

$$\|G(t,Y(t))-G(t,\overline{Y}(t))\|\leq (L_1+L_2)\|Y(t)-\overline{Y}(t)\|.$$

Consequently, $G(t,Y)$ satisfies a global Lipschitz condition in Y on the biologically feasible region.

By standard existence and uniqueness results for Caputo fractional initial-value problems, in particular, the Caputo fractional differential equation

$$D_t^{\alpha}Y(t)=G(t,Y(t)),\qquad Y(0)=Y_0,$$

has a unique solution provided $G(t,Y)$ is continuous in t and Lipschitz in Y (see, [46]) the influenza model (4) with initial conditions (3) has a unique solution. □

4 | Equilibria and its Analysis

In the absence of infection, the Disease-free Equilibirum (DFE) can be obtained upon solving model (4) for S, E, I_s, I_a, T, and R when $D_t^{\alpha}S=0$, $D_t^{\alpha}E=0$, $D_t^{\alpha}I_s=0$, $D_t^{\alpha}I_s=0$, $D_t^{\alpha}T=0$, and $D_t^{\alpha}R=0$. We obtain DFE, denoted by $\mathcal{L}_0$, which is given by

$$\mathcal{L}_0=\left(S^0,0,0,0,0,R^0\right),\tag{12}$$

where

$$S^0=\frac{\Lambda}{1-\tau+d},\quad R^0=\frac{\Lambda(1-\tau)}{(\alpha_4+d)(1-\tau+d)}.\tag{13}$$

4.1 | Basic Reproduction Number

The next-generation matrix technique considered in [47] is used to calculate the basic reproduction number for compartmental models, which methodically records the rates of new infections and the movement of individuals between disease compartments. With this method, we can express $\mathcal{R}_0$ in terms of the model parameters, giving us a crucial threshold that establishes whether the infection will disappear or continue to exist in the population. Consider η is constant, then we can obtain the following matrices:

$$F=\begin{pmatrix}0&\frac{\eta\tau S^0}{N^0}&\frac{S^0\eta\tau\kappa_1}{N^0}&\frac{S^0\eta\tau\kappa_2}{N^0}\\0&0&0&0\\0&0&0&0\\0&0&0&0\end{pmatrix},\ \text{and}$$

$$V=\begin{pmatrix}\rho_1&0&0&0\\-\delta\theta&\rho_2&0&0\\-\delta(1-\theta)&0&\rho_3&0\\0&-\phi_1&-\phi_2&\rho_4\end{pmatrix},$$

We have

$$\begin{aligned}\mathcal{R}_0^{v}&=\frac{\delta\eta_0\tau S^0\left(\theta\rho_3\left(\kappa_2\phi_1+\rho_4\right)+(1-\theta)\rho_2\left(\kappa_2\phi_2+\kappa_1\rho_4\right)\right)}{\rho_1\rho_2\rho_3\rho_4N^0},\\&=\frac{\delta\eta_0\theta S^0\tau}{\rho_1\rho_2N^0}+\frac{\delta\eta_0\theta\kappa_2S^0\tau\phi_1}{\rho_1\rho_2\rho_4N^0}+\frac{\delta\eta_0(1-\theta)\kappa_2S^0\tau\phi_2}{\rho_1\rho_3\rho_4N^0}\\&\quad+\frac{\delta\eta_0(1-\theta)\kappa_1S^0\tau}{\rho_1\rho_3N^0},\\&=\mathcal{R}_1^{v}+\mathcal{R}_2^{v}+\mathcal{R}_3^{v}+\mathcal{R}_4^{v},\end{aligned}\tag{14}$$

where R^0, and S^0 are the DFE states, and $\rho_1=d+\delta,\rho_2=\phi_1+\psi_1+\alpha_1+d,\rho_3=\phi_2+\psi_2+\alpha_2+d$, $\rho_4=\psi_3+\alpha_3+d$, and $\rho_5=\alpha_4+d$. Now, we determine the basic reproduction number without vaccine, so we put $\tau=1$, and get $S^0=\Lambda/d$, and $R^0=0$. So, we have

$$\mathcal{R}_0=\frac{\delta\eta_0\left(\theta\rho_3\left(\kappa_2\phi_1+\rho_4\right)+(1-\theta)\rho_2\left(\kappa_2\phi_2+\kappa_1\rho_4\right)\right)}{\rho_1\rho_2\rho_3\rho_4}.\tag{15}$$

The effective reproduction number $\mathcal{R}_e$ is given by

$$\mathcal{R}_e=\mathcal{R}_0\times\tau\times\frac{\eta(t)S(t)}{\eta_0N(t)},\tag{16}$$

where $\eta(t)$ is defined earlier. The model without treatment and vaccination is given by:

$$\mathcal{R}_{wtv}=\frac{\delta\eta_0}{\delta+d}\left(\frac{\theta}{\psi_1+\alpha_1+d}+\frac{(1-\theta)\kappa_1}{\psi_2+\alpha_2+d}\right),$$

and the effective seasonal reproduction number is

$$\mathcal{R}_{wtv}^{e}=\frac{\delta\eta(t)}{\delta+d}\left(\frac{\theta}{\psi_1+\alpha_1+d}+\frac{(1-\theta)\kappa_1}{\psi_2+\alpha_2+d}\right)\frac{S(t)}{N(t)}.$$

The effective reproduction number (ERN) is defined as "the average number of new infections caused by a single infected chicken in a farm where not all chickens are fully susceptible". Next, the theorem demonstrates local asymptotic stability of the DFE $\mathcal{L}_0$.

Theorem 3. *When $\mathcal{R}_0 < 1$, the fractional influenza model at $\mathcal{L}_0$ is locally asymptotically stable.*

Proof. We have Jacobian matrix (4) at $\mathcal{L}_0$ is given by,

$$J = \begin{pmatrix} -d+\tau-1 & 0 & -\frac{S^0\eta\tau}{N^0} & -\frac{S^0\eta\tau\kappa_1}{N^0} & -\frac{S^0\eta\tau\kappa_2}{N^0} & 0 \\ 0 & -\rho_1 & \frac{S^0\eta\tau}{N^0} & \frac{S^0\eta\tau\kappa_1}{N^0} & \frac{S^0\eta\tau\kappa_2}{N^0} & 0 \\ 0 & \delta\theta & -\rho_2 & 0 & 0 & 0 \\ 0 & \delta(1-\theta) & 0 & -\rho_3 & 0 & 0 \\ 0 & 0 & \phi_1 & \phi_2 & -\rho_4 & 0 \\ 1-\tau & 0 & \psi_1 & \psi_2 & \psi_3 & -\rho_5 \end{pmatrix}.$$

Here, ρ_5, and $(1-\tau)+d$ have negative real parts, whereas, to obtain the rest of the eigenvalues associated with J, we present the characteristic equation given by:

$$\lambda^4 + k_1\lambda^3 + k_2\lambda^2 + k_3\lambda + k_4 = 0, \tag{17}$$

where

$$\begin{aligned} k_1 &= \rho_1+\rho_2+\rho_3+\rho_4, \\ k_2 &= \rho_1\rho_3\big(1-\mathcal{R}_4^{\upsilon}\big) + \rho_1\rho_2\big(1-\mathcal{R}_1^{\upsilon}\big) + \rho_2\rho_3 + \big(\rho_1+\rho_2+\rho_3\big)\rho_4, \\ k_3 &= \rho_2\rho_3\rho_4 + \rho_1\rho_2\rho_3(1-\mathcal{R}_1^{\upsilon}-\mathcal{R}_4^{\upsilon}) + \rho_1\rho_2\rho_4(1-\mathcal{R}_1^{\upsilon}-\mathcal{R}_2^{\upsilon}) \\ &\quad + \rho_1\rho_3\rho_4(1-\mathcal{R}_3^{\upsilon}-\mathcal{R}_4^{\upsilon}), \\ k_4 &= \rho_1\rho_2\rho_3\rho_4(1-\mathcal{R}_0^{\upsilon}). \end{aligned}$$

Here, $k_1 > 0$, and k_4 can be positive if $\mathcal{R}_0 < 1$. Further, k_2, and k_3 also positive for $(\mathcal{R}_j < \mathcal{R}_0)$, where $j = 1,2,3,4$, which shows all the coefficients in Equation (17) are positive. Further, to guarantee stability, the Routh–Hurwitz criteria $(k_1,k_2,k_3,k_4) > 0$, and $k_1k_2k_3 > k_3^2 - k_1^2k_4$ can be easily satisfied. Hence, the Routh–Hurwitz conditions ensure that $\mathcal{L}_0$ is LAS when $\mathcal{R}_0 < 1$. □

4.2 | Endemic Equilibria

Solving the equations $D_t^{\alpha}S(t) = 0, \ldots, D_t^{\alpha}R(t) = 0$ yields the endemic equilibrium of system (4), expressed as $\mathcal{L}^* = (S^*, E^*, I_s^*, I_a^*, T^*, R^*)$, where

$$\begin{aligned} S^* &= \frac{\Lambda}{\Phi^*\tau + d - \tau + 1}, \quad E^* = \frac{\Phi^*\tau S^*}{\rho_1}, I_s^* = \frac{\delta\theta E^*}{\rho_2}, \\ I_a^* &= \frac{\delta(1-\theta)E^*}{\rho_3}, \; T^* = \frac{\phi_2 I_a^* + \phi_1 I_s^*}{\rho_4}, \\ R^* &= \frac{\psi_2 I_a^* + \psi_3 T^* + \psi_1 I^* + (1-\tau)S^*}{\rho_5}. \end{aligned}$$

Inserting the above into

$$\lambda^* = \frac{\eta\big(I_s^* + \kappa_1 I_a^* + \kappa_2 T^*\big)}{N^*}, \tag{18}$$

where $N^* = S^* + E^* + I_s^* + I_a^* + T^* + R^*$. After simplifying, we get

$$l_0\lambda^* + l_1 = 0, \tag{19}$$

where

$$\begin{aligned} l_0 &= \rho_2\tau\big(\rho_4\big(\delta(1-\theta)\psi_2 + \rho_5\big(\delta(1-\theta)+\rho_3\big)\big) \\ &\quad + \delta(1-\theta)\phi_2\big(\rho_5+\psi_3\big)\big) \\ &\quad + \delta\theta\rho_3\tau\big(\rho_4\big(\rho_5+\psi_1\big) + \phi_1\big(\rho_5+\psi_3\big)\big), \\ l_1 &= \rho_1\rho_2\rho_3\rho_4\big(1+\rho_5-\tau\big)(1-\mathcal{R}_0). \end{aligned} \tag{20}$$

From Equation (19), $l_0 > 0$, and $l_1 > 0$ if $\mathcal{R}_0 < 1$. So, $\lambda^* = -l_1/l_0$. This suggests that whenever $\mathcal{R}_0 > 1$, there is an endemic equilibrium with biological significance. Furthermore, the model (4) cannot display backward bifurcation since the system (19) is linear.

5 | Numerical Procedure and Discussion

The subsection presents the scheme for the influenza chicken disease model, and later in the subsection, we discuss the numerical results and the graphical results.

5.1 | Numerical Scheme

The fractional system considered in Equation (4) in Caputo derivative shall be solved using the detailed approach presented in the following. To do this, the Caputo fractional derivative of order $0 < \alpha \le 1$ will be solved using the fractional Adams–Bashforth type method that frequently reported for the solution of epidemic models in the literature [48–50]. We represent the system (4) in the following representations:

$$\begin{cases} {}^{C}D_t^{\alpha}\Pi(t) = \mathcal{X}(t,\Pi(t)), \\ \Pi(0) = \Pi_0, \qquad 0 < t < \tilde{T}, \end{cases} \tag{21}$$

where

$$\Pi(t) = \big(S(t), E(t), I_s(t), I_a(t), T(t), R(t)\big) \in \mathbb{R}_+^6. \tag{22}$$

Here, Π_0 represents the initial state of the system, and $\mathcal{X}(t,\Pi(t))$ is a continuous vector-valued function satisfying the Lipschitz condition. Using the Riemann–Liouville fractional integral on Equation (21), we obtain:

$$\Pi(t) = \Pi_0 + \frac{1}{\Gamma(\alpha)}\int_0^t (t-\zeta)^{\alpha-1}\mathcal{X}(\zeta,\Pi(\zeta))\,d\zeta. \tag{23}$$

Let the interval $[0,\tilde{T}]$ be uniformly divided using the step size $h = \frac{\tilde{T}}{\kappa}$, where $\kappa \in \mathbb{N}$. Following [51], we obtain the following discrete form

$$\begin{aligned} \Pi_{u+1} &= \Pi_0 + \frac{h^{\alpha}}{\Gamma(\alpha+1)}\sum_{\upsilon=0}^{u}((u-\upsilon+1)^{\alpha} - (u-\upsilon)^{\alpha})\mathcal{X}\big(t_{\upsilon},\Pi_{\upsilon}\big), \\ &\quad u = 0,1,\ldots,\kappa-1. \end{aligned} \tag{24}$$

Substituting (24) into the fractional influenza system (4), the fractional difference scheme becomes

$$
\begin{aligned}
S_{u+1} &= S_0 + g_1 \sum_{v=0}^{u} x_{u,v}\left[\Lambda - \tau\Phi_v S_v - (1-\tau)S_v - dS_v\right],\\
E_{u+1} &= E_0 + g_1 \sum_{v=0}^{u} x_{u,v}\left[\tau\Phi_v S_v - \delta E_v - dE_v\right],\\
I_{su+1} &= I_{s0} + g_1 \sum_{v=0}^{u} x_{u,v}\left[\theta\delta E_v - (\phi_1+\psi_1+\alpha_1+d)I_{sv}\right],\\
I_{au+1} &= I_{a0} + g_1 \sum_{v=0}^{u} x_{u,v}\left[(1-\theta)\delta E_v - (\phi_2+\psi_2+\alpha_2+d)I_{av}\right],\\
T_{u+1} &= T_0 + g_1 \sum_{v=0}^{u} x_{u,v}\left[\phi_1 I_{sv} + \phi_2 I_{av} - (\psi_3+\alpha_3+d)T_v\right],\\
R_{u+1} &= R_0 + g_1 \sum_{v=0}^{u} x_{u,v}\\
&\quad \left[\psi_1 I_{sv} + \psi_2 I_{av} + \psi_3 T_v + (1-\tau)S_v - (\alpha_4+d)R_v\right],
\end{aligned}
\tag{25}
$$

where

$$
g_1 = \frac{h^\alpha}{\Gamma(\alpha+1)}, \qquad x_{u,v} = (u-v+1)^\alpha - (u-v)^\alpha,
$$

and

$$
\Phi_v = \frac{\eta(t_v)(I_{sv} + \kappa_1 I_{av} + \kappa_2 T_v)}{N_v},
$$

where

$$
N_v = S_v + E_v + I_{sv} + I_{av} + T_v + R_v.
$$

5.2 | Numerical Simulation

Here, we present the simulation of the model (4) considering the effective scheme presented in Equation (25). The numerical values of the parameters used in the numerical simulation are presented in Table 1, where some are taken from existing literature, while the remaining parameters are fitted to the data using nonlinear least squares. In Figure 2b, the seasonal ERN $\mathcal{R}_e$ under different cases is considered. We consider no intervention, treatment only, treatment plus vaccination only, and vaccination only with 80% efficacy. When there is no intervention, the ERN fluctuates above unity due to seasonal variations, which indicates the potential for the disease to spread. Only using the treatment reduces ERN, but it still occasionally exceeds the epidemic threshold. Considering vaccine efficacy only, and its combination with treatment, greatly reduces the ERN below unity. The results show that a highly effective vaccine can better control the disease outbreak, even in the absence of treatment, while the combination achieves the greatest reduction in transmission. In Figure 3, we provide the comparison of real data versus model solution, symptomatic infected chicken, and their respective residual. We observe that the data is fit well to the real data obtained from the source [7, 52] for the influenza outbreak in Bangladesh, Dhaka City Corporation, for the period September 2016 to August 2018. The initial condition used in data fitting is $S(0) = 175,620,100,$

TABLE 1 | Description of parameters and their values used in the numerical simulations.

Notation	Definition	Numerical value	References	Unit
κ_1	Coefficient for asymptomatic individuals	0.7–0.8	[13]	—
κ_2	Coefficient for treated individuals	0.6	[53]	—
$1-\tau$	Vaccine efficiency rate	0.8–1	[54]	—
δ	Incubation rate	0.05–0.5	[55]	month^{-1}
$1-\theta$	Proportion of exposed individuals who develop asymptomatic infection	0.05–0.35	[56]	—
ϕ_1	Treatment of symptomatic individuals	0.7–0.9	[13]	month^{-1}
ϕ_2	Treatment of asymptomatic individuals	0.7–0.9	[13]	month^{-1}
ψ_1	Recovery rate of infected individuals	0–0.1	[57]	month^{-1}
ψ_2	Recovery rate of asymptomatic individuals	0.6	[56]	month^{-1}
ψ_3	Rate of recovery of treated individuals	0.7	[58]	month^{-1}
α_1	Death rate of infected individuals	0.9–1	[57]	month^{-1}
α_2	Mortality rate of asymptomatic individuals	0.7–0.8	[58]	month^{-1}
α_3	Death rate of treated individuals	0.6	[59]	month^{-1}
α_4	Death rate of recovered individuals	0.1	[52]	month^{-1}
d	Natural death rate	0.000	—	month^{-1}
Λ	Recruitment rate	0.00	—	month^{-1}
η	Contact rate	$\eta_1 \in [0,1]$	Variable	month^{-1}
η_0	Constant contact rate	9.9762×10^{-1}	Fitted	month^{-1}
η_1	Degree of seasonality	0.4815	Fitted	—
ν	Initial phase of the amplitude	$\pi/6$	—	—

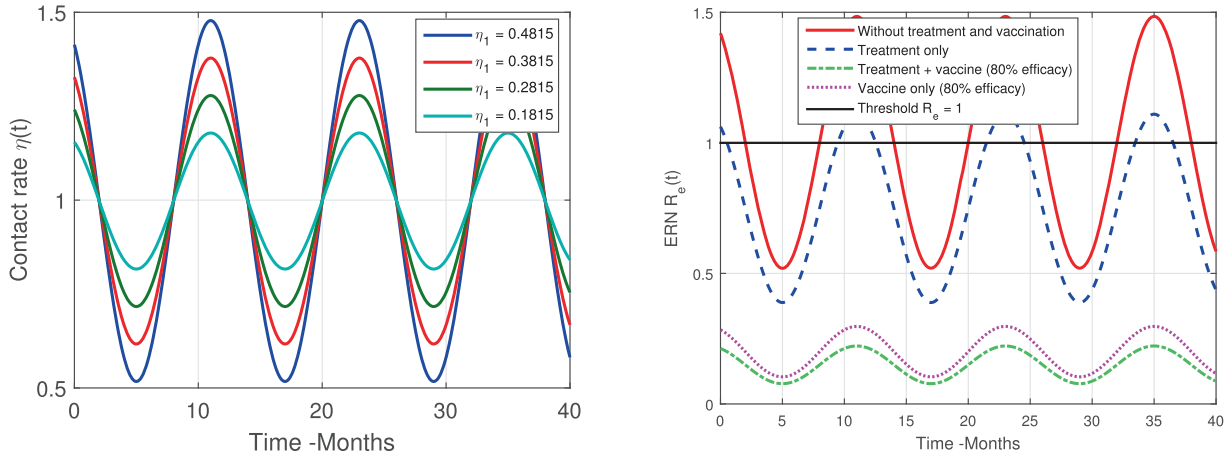

FIGURE 2 | The plot represents the contact rate η and the ERN for different cases: (a) represents the contact rate η for various values $\eta_1 = (0.5116, 0.3116, 0.1116)$, and in (b) the ERN is presented for various cases.

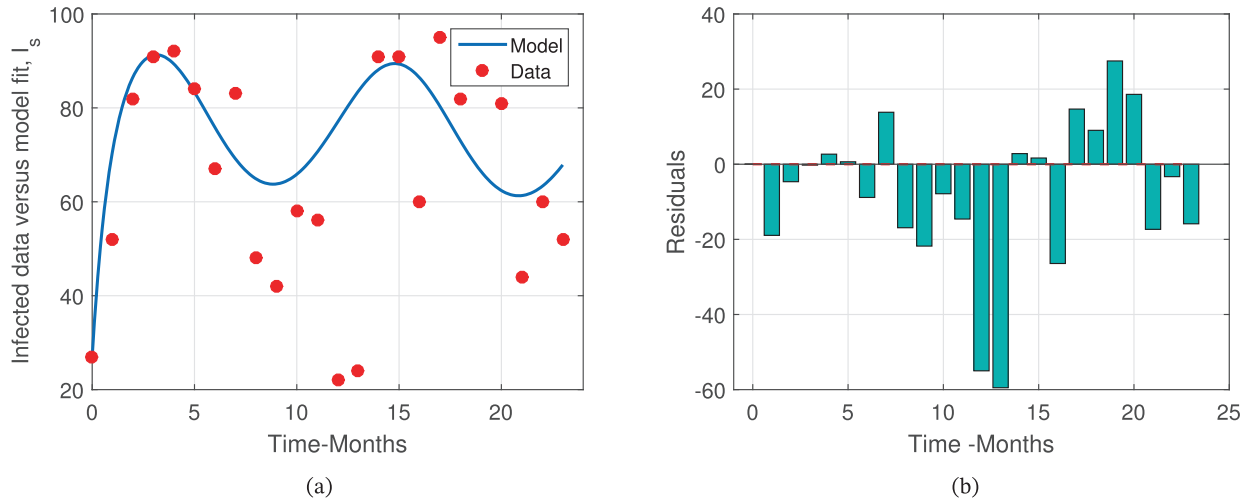

FIGURE 3 | The plot compares the actual data with the model predictions. (a) shows the data versus the model, while (b) displays the residuals.

$E(0) = 460$, $I_s = 27$, $(I_a, T, R) = (0, 0, 0,)$. We also point out that in data fitting, we consider the model fitig without treatmnet and wotuout vaccination, so $\phi_1 = 0, \phi_2 = 0, \alpha_3 = 0, \kappa_2 = 0, \Lambda = 0$, $d = 0$, and $\tau = 1$. The graphical representation of the function $\eta(t)$ for the given values is presented in Figure 2a.

The fitting-related results, such as RMSE: 21.3390, MAE: 15.1123, and R^2: 0.1434 were computed. We estimated the basic reproduction number with no vaccine and treatment is $\mathcal{R}_{wtv} = 1.002$ while without vaccination but with treatment, we get $\mathcal{R}_0 = 0.75$. Figure 4 represents the comparison of real data and predicted data. This is a clear look hows the predicted data is close to the real monthly cases. We see in Figure 4b, that when $\alpha = 0.8$, the comparison looks better.

Figure 5 is presented to study the dynamical behavior of exposed, infected, and asymptomatic compartments for the case with and without treatment and vaccination. We observe that vaccination has a meaningful impact on the disease and recommend vaccinating all chickens to get better results for the farmers.

Figure 6 is given to show the dynamical behavior of exposed, symptomatic, asymptomatic, and recovered populations for various values of the degree of seasonality η_1, while keeping the fractional order fixed at $\alpha = 0.9$. Larger values of η_1 give stronger seasonal effects and produce higher peaks in exposed, symptomatic, and asymptomatic populations. When decreasing η_1, the seasonal peaks become smaller, and thus weaker transmission and stable growth in the recovered population occur. Moreover, higher values of η_1 show rapid disease spread and cause sharp outbreaks in the chicken populations of exposed, symptomatic, and asymptomatic, while lower values of η_1 lead to smaller outbreaks and steadier disease spread. Implementing vaccination, biosecurity, and other appropriate control measures reduces losses in the flock.

Figure 7 presents the dynamics of exposed, symptomatic, and asymptomatic populations for various values of the fractional-order α. We observe that decreasing α leads to the emergence of seasonal behavior. When the fractional order α decreases, the amplitude of seasonal oscillations in exposed,

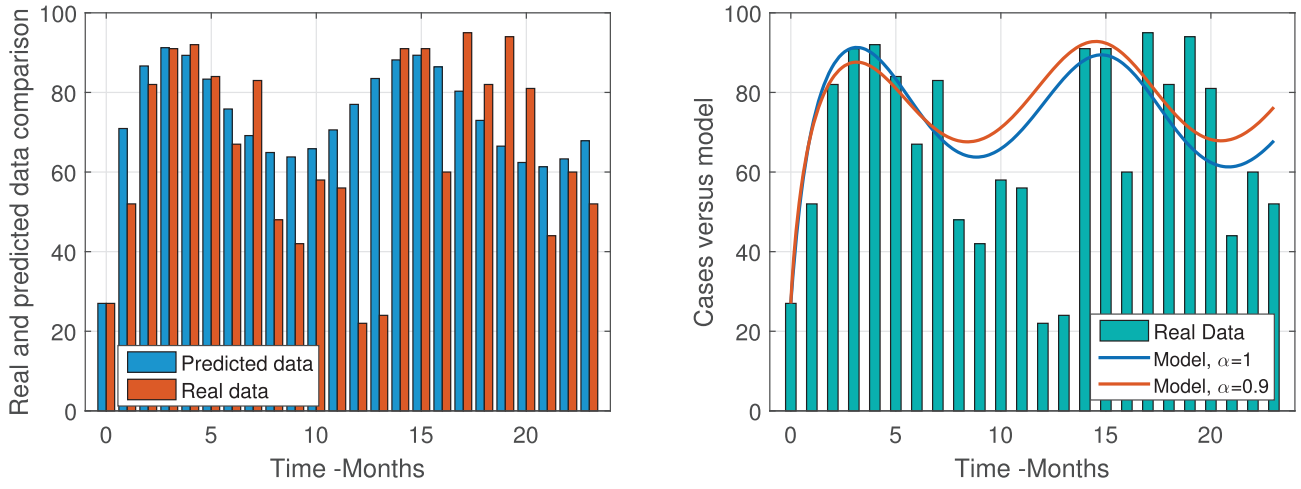

FIGURE 4 | The comparison of real data via bar graph is given in (a), while (b) is their respective result for fractional case $\alpha = 0.8$.

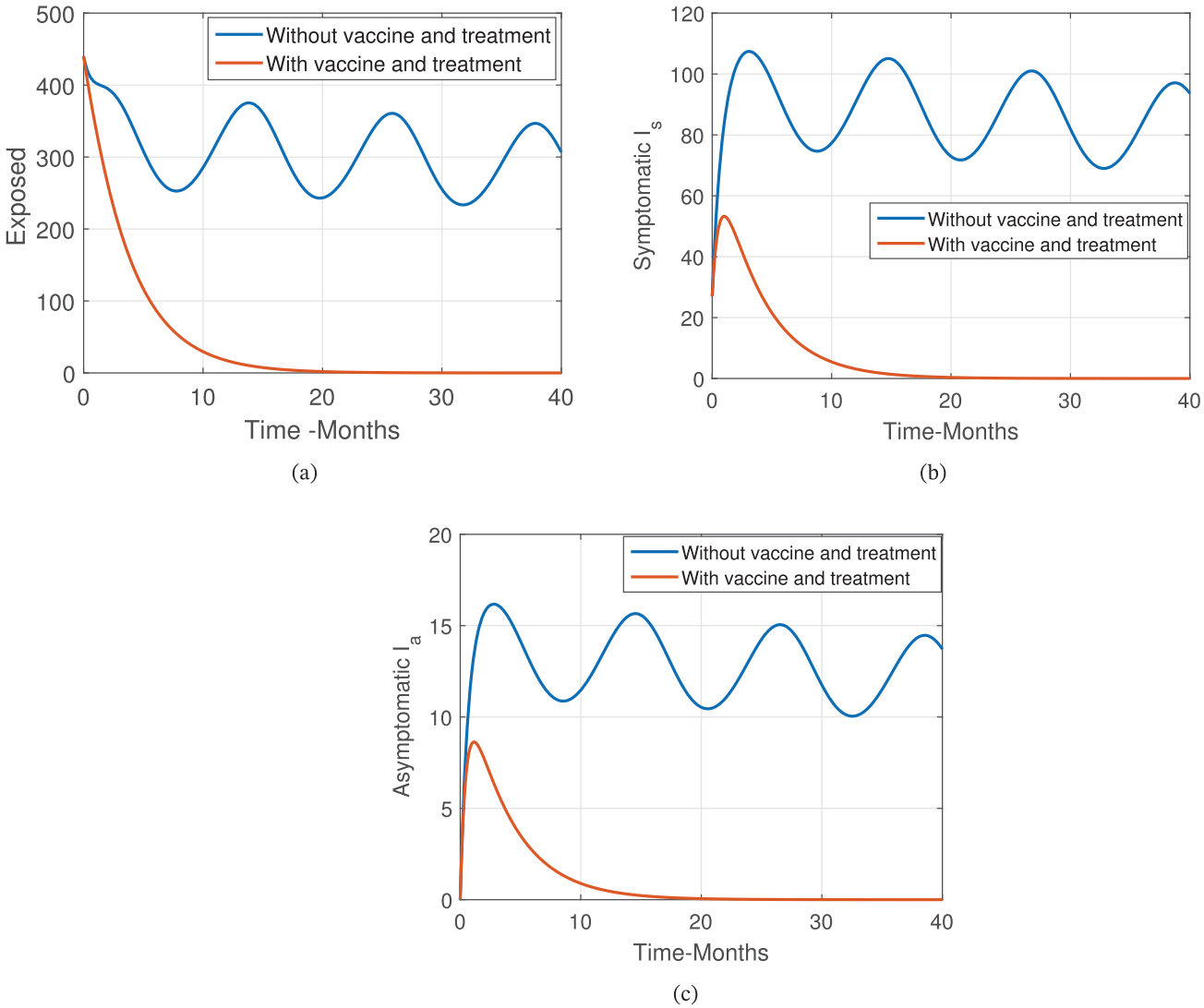

FIGURE 5 | The plot represents the comparison of the model without treatment and vaccine. With treatment and vaccine $\tau = 0.2$, $\psi_3 = 0.7$, $\phi_1 = \phi_2 = 0.8$, $\kappa_2 = 0.6$ while for with vaccine and treatment, $\tau = 1$, $\psi_3 = 0$, $\phi_1 = \phi_2 = 0$, $\kappa_2 = 0$.

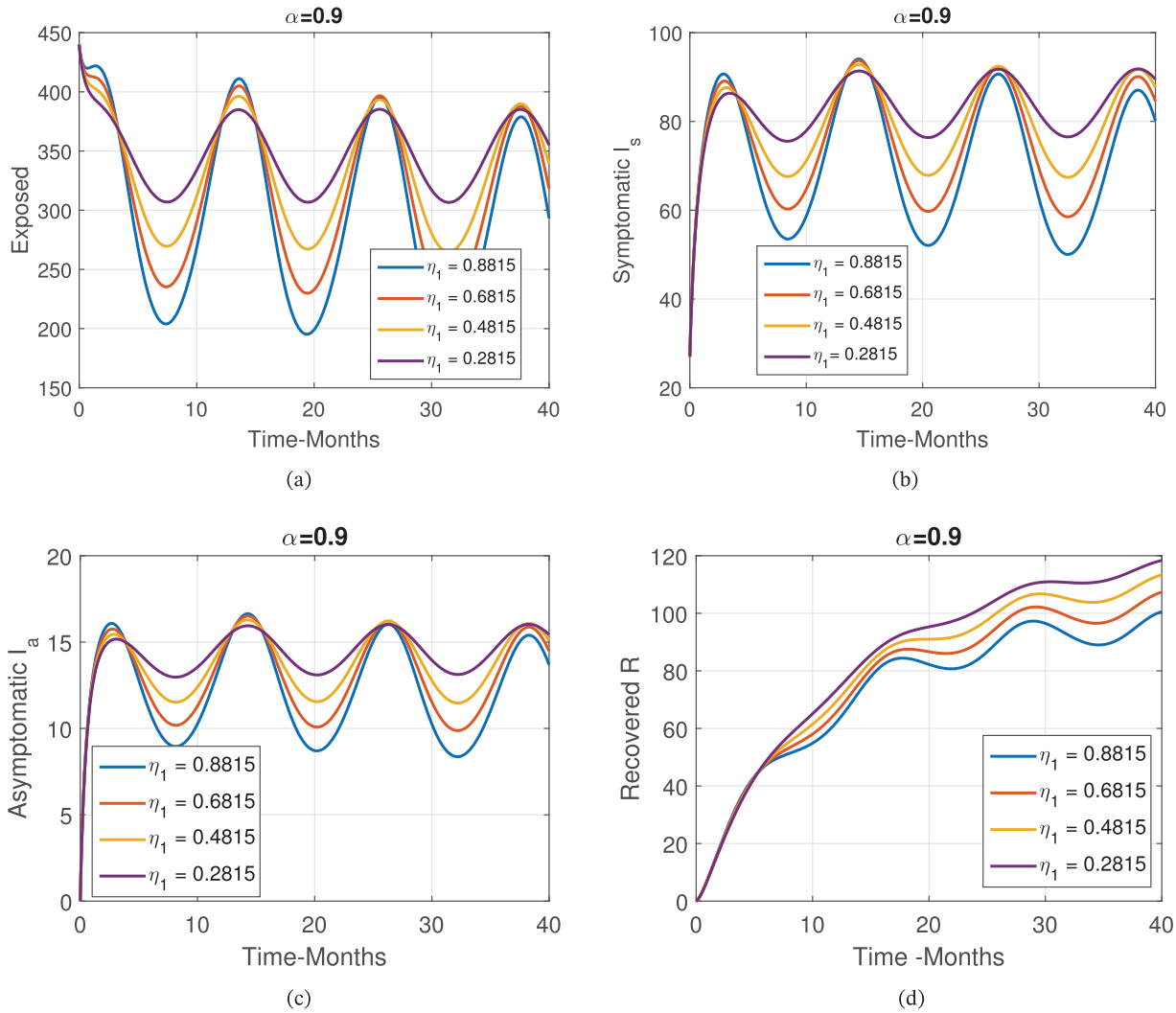

FIGURE 6 | Dynamical behavior of exposed, symptomatic, asymptomatic, and recovered population for various values of $\eta_1 = (0.8815, 0.6815, 0.4815, 0.2815)$ when $\alpha = 0.9$.

symptomatic, and asymptomatic chicken populations increases. Small values of α give higher peaks and more pronounced fluctuations over time. This indicates that memory effects significantly influence disease dynamics in the flock.

Figure 8 shows the dynamics of exposed, symptomatic, asymptomatic, and treated chicken populations for various values of τ, where the vaccine efficacy is 1-τ. When τ decreases from 1 to 0.4 (an increase in vaccine efficacy), the population sizes of all infected compartments and the treatment population increase. Reducing the vaccine inefficacy leads to better control of the disease and reduces the number of infected and treated individuals in the flock. So, it is recommended to vaccinate the chicken using vaccines with efficacy rates to minimize losses in the flock.

Figure 9a–d shows the impact of four degrees of seasonality on the population of exposed, symptomatic, asymptomatic, and treated individuals.

Figure 10 is presented to show the dynamics of exposed, symptomatic, asymptomatic, and treated individuals when fixing $\alpha = 0.9$ and varying κ_1. We observe a decrease in these infected compartments when decreasing the contact rate κ_1. Similarly Figure 11 is given to show the impact of κ_2 on the infected model compartments when $\alpha = 0.9$ and varying $\kappa_2 = 0.8, 0.6, 0.4$.

Figure 12 shows the comparison of fractional and integer order phase portraits of susceptible versus exposed, and exposed versus symptomatic infected for different values of η_1 and fixed fractional order $\alpha = 0.86$.

Figure 13 shows the comparison of fractional and integer order phase portraits of susceptible versus exposed, and exposed versus symptomatic infected for different values of τ and fixed fractional order $\alpha = 0.86$.

The numerical results presented above show how the influenza infection spreads and persists in chicken farms under certain biological conditions. It follows from the results that the infection progresses follow a seasonal exposure, immunity development, and the presence of both symptomatic and asymptomatic birds. In higher contact periods, many chickens progress into exposed and infected classes, leading to noticeable outbreak peaks. Vaccination has a great role in lowering vulnerability and overall

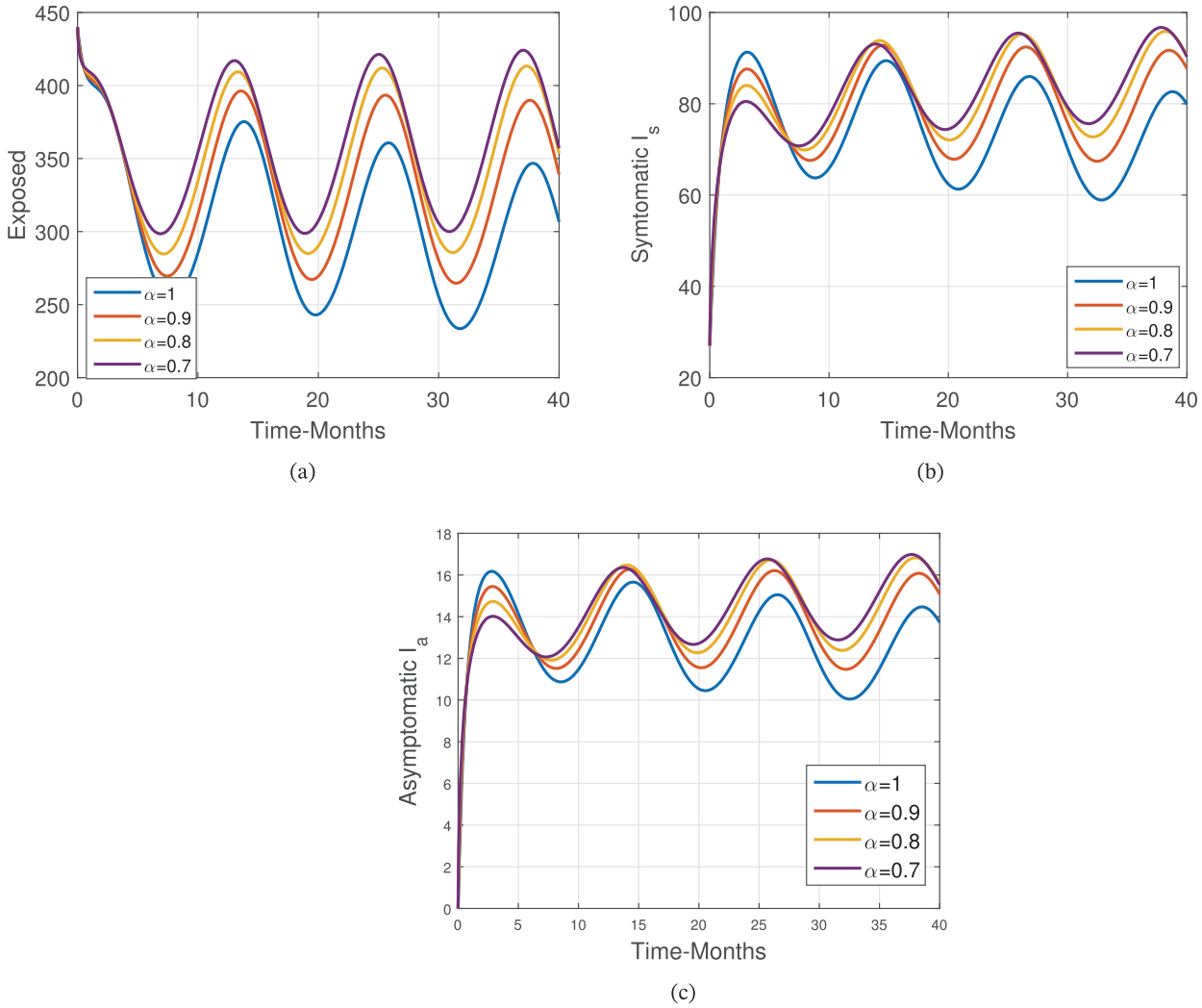

FIGURE 7 | The dynamical behavior of exposed, symptomatic, and asymptomatic individuals when $\alpha = 1, 0.9, 0.8, 0.7$ are given respectively in sub-figures (a) to (c).

infection pressure in the flock. Treating the infected chickens also helps to control and shorten the disease and limit further spread. The more important is, the asymptomatic chicken, which is a hidden source of infection, may explain repeated outbreaks even when visible cases decline. These findings underline the importance of combining vaccination, treatment, and seasonal biosecurity measures to effectively manage avian influenza in poultry farms.

6 | Conclusion

In the present study, we investigated the dynamics of a chicken fractional influenza model under real data. Using the standard incidence rate, the classical model formulation is provided. We then extended the model into a fractional order version using the Caputo derivative. We showed that the influenza fractional order model is non-negative and uniformly bounded. Further, we proved that the chicken fractional influenza disease model admits a unique solution. The equilibrium point associated with the influenza fractional model for $\mathcal{R}_0 < 1$ at the DFE $\mathcal{L}_0$ is analyzed and found to be locally asymptotically stable. The expression for the endemic equilibrium is obtained, and a unique endemic equilibrium $\mathcal{L}^*$ is found for the model. To obtain the numerical results, we first provided a general procedure for numerically solving the fractional differential equation in the Caputo case, and then derived a scheme for our model. We solved the model and obtained various graphical results. The seasonality involved in the model has been fitted using nonlinear least squares fitting, while the values of the other parameters were taken from the literature. We obtained the numerical value for the basic reproduction number $\mathcal{R}_0 = 0.75$. We provided the real data monthly in various plots and showed that the fractional order results are better. A case with and without vaccination and treatment is provided, and found that the vaccination with high efficacy provided better results for disease elimination. The effect of vaccine efficacy on the infected compartments is illustrated, showing a more pronounced decrease in infections. The effect of contact rates and the fractional order α for different values provides graphical results that are beneficial for disease elimination.

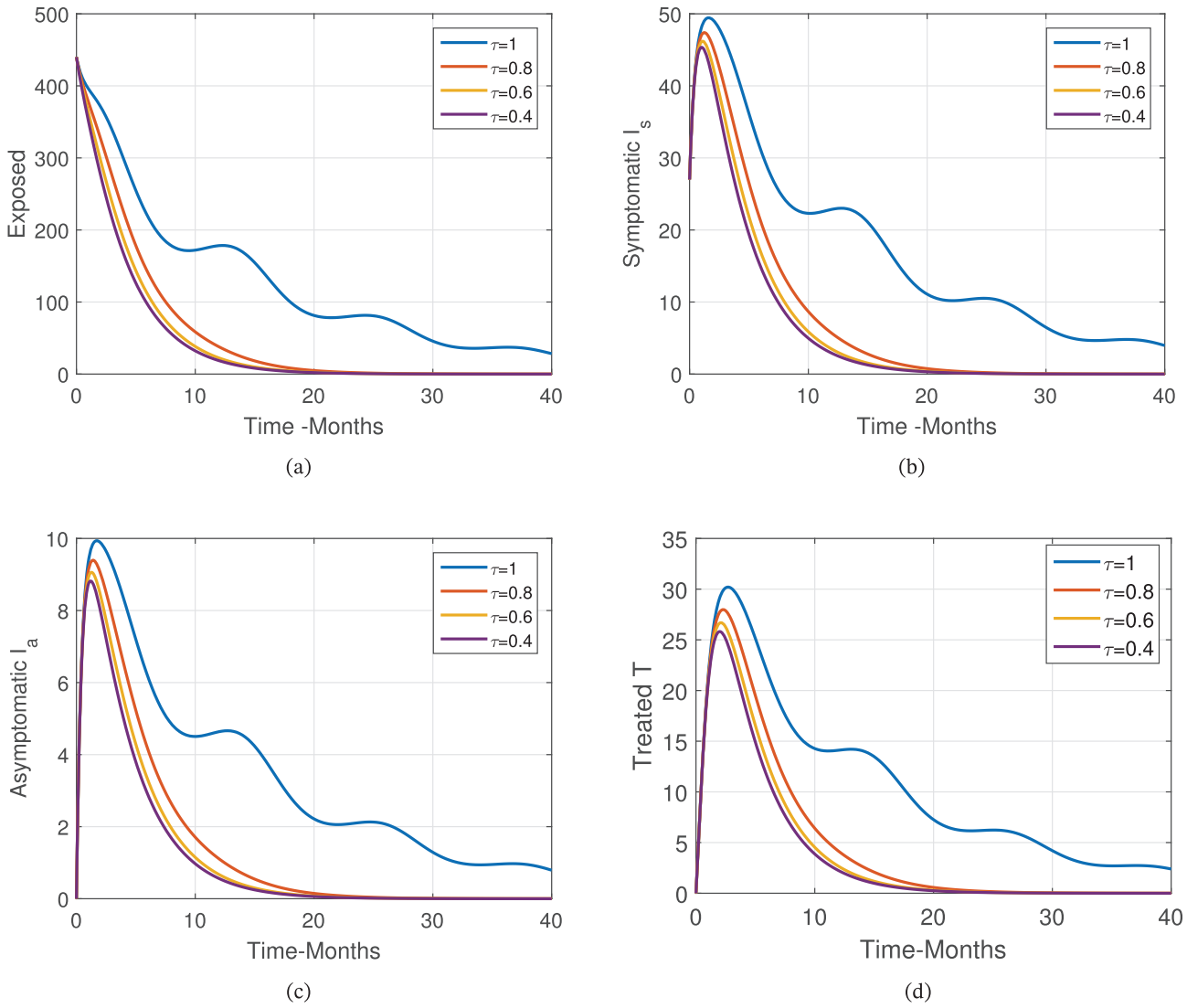

FIGURE 8 | The effects of vaccine inefficacy on the infected and treated populations are shown in sub-figures (a) to (d), respectively.

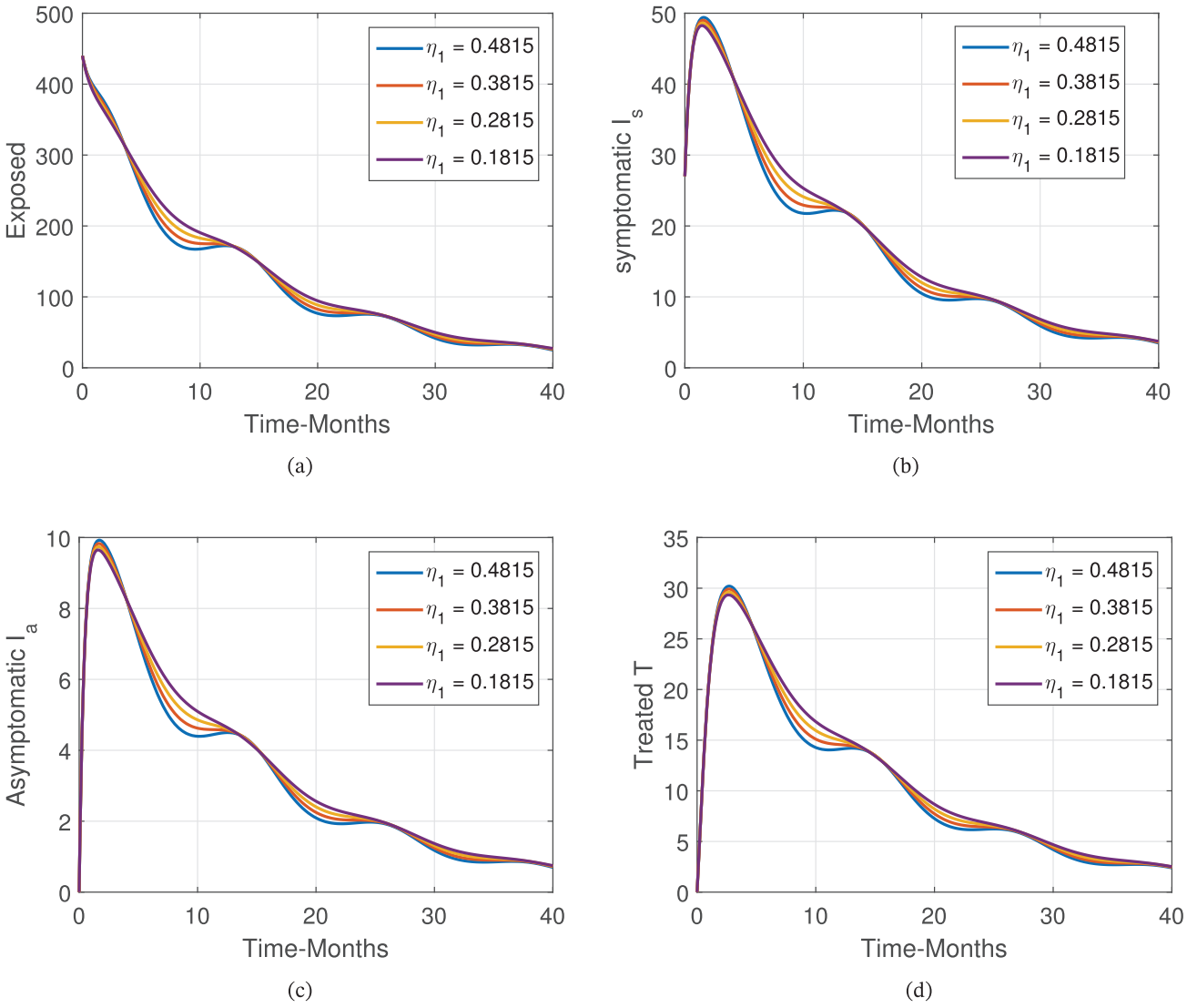

FIGURE 9 | The impact of degree of seasonality on infected compartments on the model for $\eta_1 = 0.4815, 0.3815, 0.2815, 0.1815$.

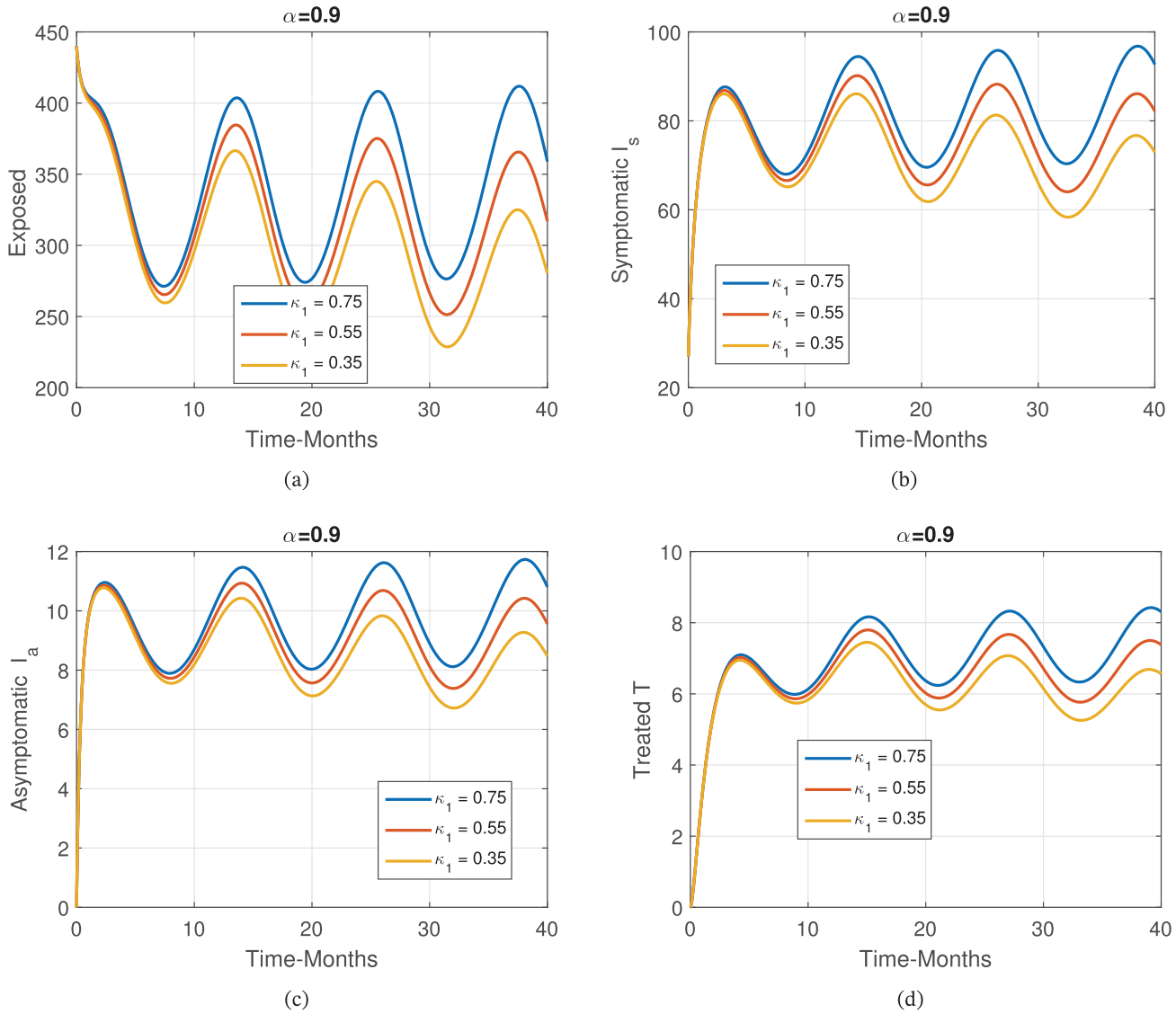

FIGURE 10 | The effect of contact parameter κ_1 on the infected and treated populations shown respectively in sub-figures (a) to (d).

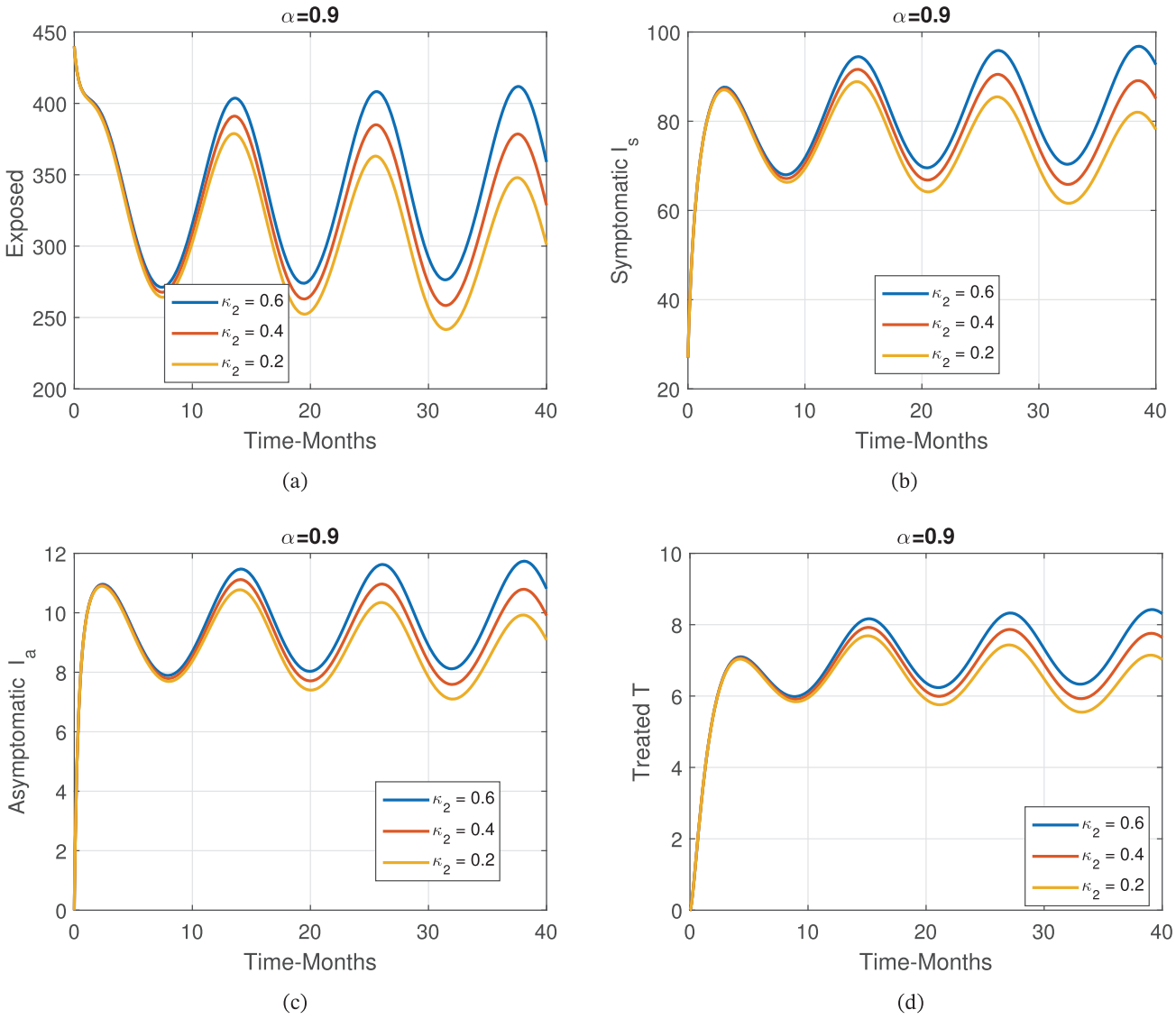

FIGURE 11 | The effect of contact parameter κ_2 on the infected and treated population given respectively in sub-figures (a) to (d).

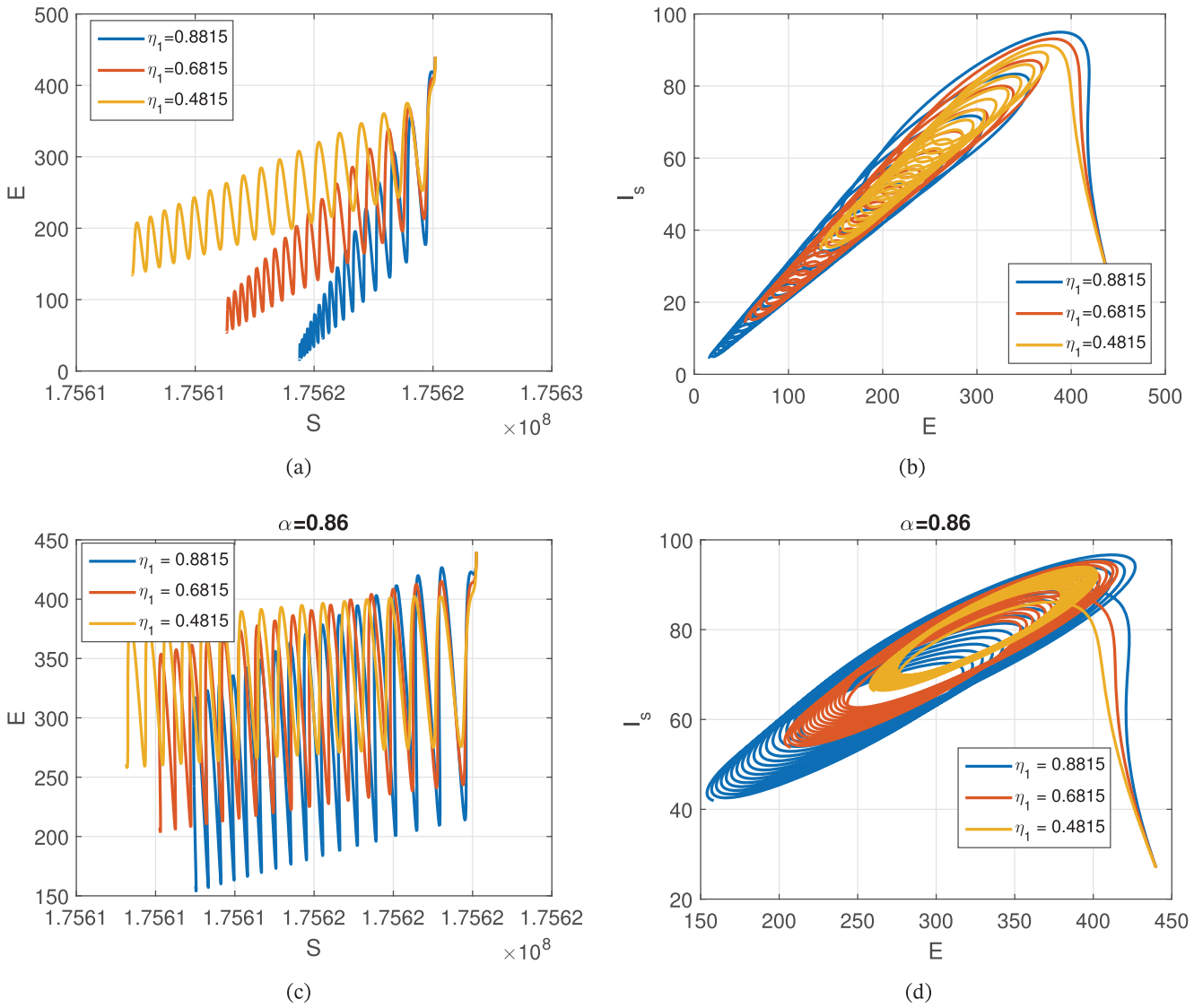

FIGURE 12 | Phase portraits of S and E, and, E and I_s for $\eta_1 = 0.8815, 0.86815, 0.4815$ values are shown in (a) and (b) respectively, while the phase portraits of S and E, and E and I_s for $\eta_1 = 0.8815, 0.86815, 0.4815$ values are given in (c) and (d) respectively, for fixed $\alpha = 0.86$.

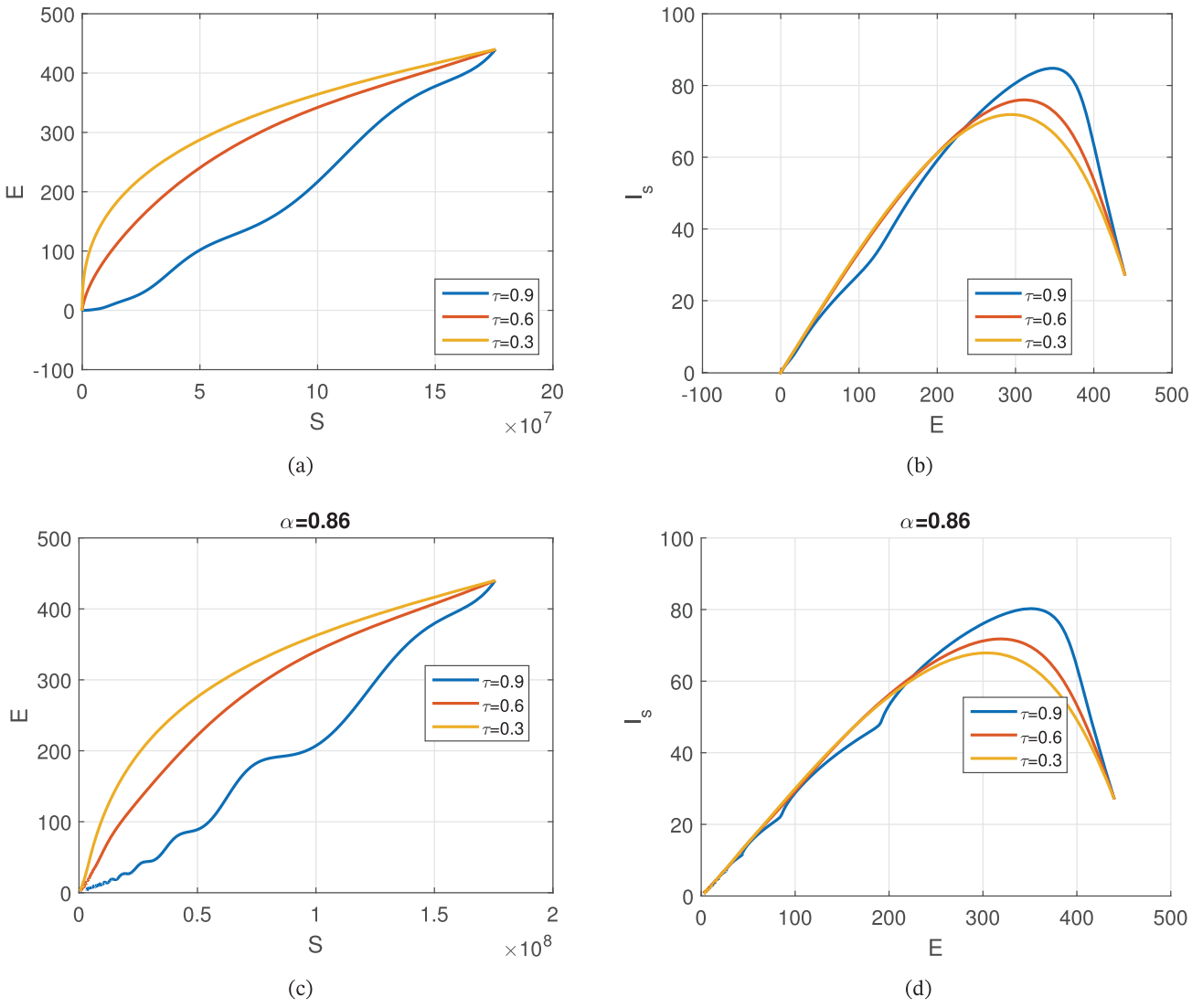

FIGURE 13 | Phase portraits of S and E, and E and I_s for $\tau = 0.9, 0.6, 0.3$ shown (a) and (b) respectively, while the phase portraits of S and E, and E and I_s for $\tau = 0.9, 0.6, 0.3$ and $\alpha = 0.86$, respectively in sub-figures (c) and (d).

The ERN, $\mathcal{R}_e$ with different scenarios, is presented, which shows the importance of disease control. We observe fluctuation above unity in $\mathcal{R}_e$ when there is no treatment and vaccination, which shows the disease spreads in the farms. When considering only the treatment that reduces ERN, but it still crosses the unity and fluctuates. Taking without treatment, and 80% vaccine efficacy, we get a lower ERN, and make it significantly below unity, which shows the results are better even with no treatment but with a good efficacy rate. The most important case is the combined treatment plus 80% vaccine efficacy that reduces consistent ERN below unity, which is the strongest reduction in transmission. It should be noted that with all these scenarios, there is still the seasonal effect, but its impact is highly reduced when effective interventions are applied.

Author Contributions

All authors contributed equally in the preparation of the manuscript and its final submission.

Acknowledgments

The authors are thankful to the Deanship of Research and Graduate Studies, King Khalid University, Abha, Saudi Arabia, for financially supporting this work through the Large Research Group Project under Grant No. R.G.P.2/504/46.

No AI tools, such as ChatGPT has been used in the preparation of the manuscript except for grammar correction.

Funding

The authors are thankful to the Deanship of Research and Graduate Studies, King Khalid University, Abha, Saudi Arabia, for financially supporting this work through the Large Research Group Project under Grant No. R.G.P.2/504/46.

Conflicts of Interest

The authors declare no conflicts of interest.

Data Availability Statement

The data reported in this study are inside the manuscript in the references [7, 52].

References

1. H.-N. Gao, H.-Z. Lu, B. Cao, et al., "Clinical Findings in 111 Cases of Influenza A (H7N9) Virus Infection," *New England Journal of Medicine* 368, no. 24 (2013): 2277–2285.

2. J. L. Gonzales, S. Pritz-Verschuren, R. Bouwstra, J. Wiegel, A. R. W. Elbers, and N. Beerens, "Seasonal Risk of Low Pathogenic Avian Influenza Virus Introductions Into Free-Range Layer Farms in The Netherlands," *Transboundary and Emerging Diseases* 68, no. 1 (2021): 127–136.

3. C. G. von Waldburg-Zeil, N. van Staaveren, and A. Harlander-Matauschek, "Do Laying Hens Eat and Forage in Excreta From Other Hens?," *Animal* 13, no. 2 (2019): 367–373.

4. K. Dietze, A. Graaf, T. Homeier-Bachmann, et al., "From Low to High Pathogenicity?Characterization of H7N7 Avian Influenza Viruses in Two Epidemiologically Linked Outbreaks," *Transboundary and Emerging Diseases* 65, no. 6 (2018): 1576–1587.

5. J. L. Gonzales and A. R. W. Elbers, "Effective Thresholds for Reporting Suspicions and Improve Early Detection of Avian Influenza Outbreaks in Layer Chickens," *Scientific Reports* 8, no. 1 (2018): 8533.

6. Y. Xing, L. Song, G.-Q. Sun, Z. Jin, and J. Zhang, "Assessing Reappearance Factors of H7N9 Avian Influenza in China," *Applied Mathematics and Computation* 309 (2017): 192–204.

7. I. Berry, M. Rahman, M. S. Flora, et al., "Seasonality of Influenza and Coseasonality With Avian Influenza in Bangladesh, 2010–19: A Retrospective, Time-Series Analysis," *Lancet Global Health* 10, no. 8 (2022): e1150–e1158.

8. B. K. Mishra and D. N. Sinha, "A Mathematical Model on Avian Influenza With Quarantine and Vaccination," *Journal of Immunological Techniques & Infectious Diseases* 5, no. 4 (2016): 2.

9. J. Zhang, Y. Li, Z. Jin, and H. Zhu, "Dynamics Analysis of an Avian Influenza A (H7N9) Epidemic Model With Vaccination and Seasonality," *Complexity* 2019, no. 1 (2019): 4161287.

10. E. M. Hill, T. House, M. S. Dhingra, et al., "Modelling H5N1 in Bangladesh Across Spatial Scales: Model Complexity and Zoonotic Transmission Risk," *Epidemics* 20 (2017): 37–55.

11. Y. Hayama, K. Sawai, M. Yoshinori, E. Yamaguchi, and T. Yamamoto, "Estimation of Introduction Time Window of Highly Pathogenic Avian Influenza Virus Into Broiler Chicken Farms During the 2020–2021 Winter Season Outbreak in Japan," *Preventive Veterinary Medicine* 208 (2022): 105768.

12. T. Zheng, L. Nie, H. Zhu, Y. Luo, and Z. Teng, "Role of Seasonality and Spatial Heterogeneity in the Transmission Dynamics of Avian Influenza," *Nonlinear Analysis: Real World Applications* 67 (2022): 103567.

13. A. Malek and A. Hoque, "Mathematical Modeling of Bird Flu With Vaccination and Treatment for the Poultry Farms," *Comparative Immunology, Microbiology and Infectious Diseases* 80 (2022): 101721.

14. C. D. Harvell, C. E. Mitchell, J. R. Ward, et al., "Climate Warming and Disease Risks for Terrestrial and Marine Biota," *Science* 296, no. 5576 (2002): 2158–2162.

15. S. Altizer, A. Dobson, P. Hosseini, P. Hudson, M. Pascual, and P. Rohani, "Seasonality and the Dynamics of Infectious Diseases," *Ecology Letters* 9 (2006): 467–484.

16. J. L. Aron and I. B. Schwartz, "Seasonality and Period-Doubling Bifurcations in an Epidemic Model," *Journal of Theoretical Biology* 110, no. 4 (1984): 665–679.

17. W. P. London and J. A. Yorke, "Recurrent Outbreaks of Measles, Chickenpox and Mumps. I. Seasonal Variation in Contact Rates," *American Journal of Epidemiology* 98, no. 6 (1973): 453–468.

18. K. Dietz, "The Incidence of Infectious Diseases Under the Influence of Seasonal Fluctuations," in *Mathematical Models in Medicine* (Springer, 1976), 1–15.

19. J. Greenman, M. Kamo, and M. Boots, "External Forcing of Ecological and Epidemiological Systems: A Resonance Approach," *Physica D: Nonlinear Phenomena* 190 (2004): 136–151.

20. N. C. Grassly and C. Fraser, "Seasonal Infectious Disease Epidemiology," *Proceedings of the Royal Society B: Biological Sciences* 273, no. 1600 (2006): 2541–2550.

21. H. W. Hethcote, "Qualitative Analyses of Communicable Disease Models," *Mathematical Biosciences* 28, no. 3–4 (1976): 335–356.

22. A. Apisarnthanarak, R. Kitphati, K. Thongphubeth, et al., "Atypical Avian Influenza (H5N1)," *Emerging Infectious Diseases* 10, no. 7 (2004): 1321–1324.

23. D.-H. Lee, Y.-N. Lee, J.-K. Park, et al., "Antiviral Efficacy of Oseltamivir Against Avian Influenza Virus in Avian Species," *Avian Diseases* 55, no. 4 (2011): 677–679.

24. S. Meng, L. Yang, C. Xu, et al., "Recombinant Chicken Interferon-α Inhibits H9N2 Avian Influenza Virus Replication in Vivo by Oral Administration," *Journal of Interferon & Cytokine Research* 31, no. 7 (2011): 533–538.

25. K. E. Goossens, A. C. Ward, J. W. Lowenthal, and A. G. D. Bean, "Chicken Interferons, Their Receptors and Interferon-Stimulated Genes," *Developmental & Comparative Immunology* 41, no. 3 (2013): 370–376.

26. N. Barjesteh, K. O'Dowd, and S. M. Vahedi, "Antiviral Responses Against Chicken Respiratory Infections: Focus on Avian Influenza Virus and Infectious Bronchitis Virus," *Cytokine* 127 (2020): 154961.

27. Z. U. A. Zafar, M. A. Khan, A. Akgül, M. Asiri, and M. B. Riaz, "The Analysis of a New Fractional Model to the Zika Virus Infection With Mutant," *Heliyon* 10, no. 1 (2024): eXXXX.

28. A. Kumar, A. Prakash, and H. M. Baskonus, "The Epidemic COVID-19 Model via Caputo–Fabrizio Fractional Operator," *Waves in Random and Complex Media* 35, no. 4 (2025): 6230–6244.

29. Abayneh Kebede Fantaye, "Fractional Order for the Transmission Dynamics of Coffee Berry Diseases (CBD)," *European Journal of Applied Mathematics* 36, no. 4 (2025): 879–896.

30. K. Shah, T. Abdeljawad, and Z. Ali, "Mathematical Model and Simulations of Fractional Order for an Infectious Disease Involving Social Media," *Modeling Earth Systems and Environment* 11, no. 6 (2025): 1–16.

31. B. Mohammadaliee, M. E. Samei, V. Roomi, and S. Rezapour, "Optimal Control Strategies and Cost-Effectiveness Analysis for Infectious Diseases Under Fractal-Fractional Derivative: A Case Study of Cholera Outbreak. B. Mohammadaliee," *Journal of Applied Mathematics and Computing* 71, no. 3 (2025): 4197–4226.

32. D. Prathumwan, I. Chaiya, and K. Trachoo, "Analysis of an ABC-Fractional Asset Flow Model for Financial Markets," *Fractal and Fractional* 9, no. 9 (2025): 563.

33. K. Trachoo, I. Chaiya, S. Phakmee, and D. Prathumwan, "Dynamics of Bone Remodeling by Using Mathematical Model Under ABC Time-Fractional Derivative," *Symmetry* 17, no. 6 (2025): 905.

34. A. K. Sinha and K. Soni, "Fractional-Order Modeling of Hepatitis B Dynamics Incorporating Socio-Environmental Factors," *Discover Public Health* 22, no. 1 (2025): 537.

35. A. Pandey and S. Ghosh, "Dynamical Analysis of a Fractional-Order Influenza Model With Stability and Control Perspectives," *Engineering Computations* (2025): 1–36.

36. G. K. Hailu, S. W. Teklu, and D. K. Mamo, "Modeling and Analyzing the Addiction of Gambling Through Fractional Calculus With Optimal Control Strategies," *International Journal of Mathematics and Mathematical Sciences* 2025, no. 1 (2025): 2092650.

37. S. Paul, A. Mahata, S. Mukherjee, P. C. Mali, and B. Roy, "Fractional Order SEIQRD Epidemic Model of COVID-19: A Case Study of Italy," *PLoS One* 18, no. 3 (2023): e0278880.

38. S. Paul, A. Mahata, M. Karak, S. Mukherjee, S. Biswas, and B. Roy, "A Fractal-Fractional Order Susceptible-Exposed-Infected-Recovered (SEIR) Model With Caputo Sense," *Healthcare Analytics* 5 (2024): 100317.

39. S. Paul, A. Mahata, S. Mukherjee, S. K. Mahato, M. Salimi, and B. Roy, "Study of Fuzzy Fractional Caputo Order Approach to Diabetes Model," in *Fuzzy Optimization, Decision-Making and Operations Research: Theory and Applications* (Springer, 2023), 423–434.

40. S. Paul, A. Mahata, M. Karak, S. Mukherjee, S. Biswas, and B. Roy, "Dynamical Behavior of Fractal-Fractional Order Monkeypox Virus Model," *Franklin Open* 7 (2024): 100103.

41. S. Paul, A. Mahata, S. Mukherjee, et al., "Study of Fractional Order SIR Model With MH Type Treatment Rate and Its Stability Analysis," *Bulletin of Biomathematics* 2, no. 1 (2024): 85–113.

42. I. Podlubny, *Fractional Differential Equations: An Introduction to Fractional Derivatives, Fractional Differential Equations, to Methods of Their Solution and Some of Their Applications* (Elsevier, 1998).

43. R. Almeida, M. C. Artur, B. da Cruz, N. Martins, M. Teresa, and T. Monteiro, "An Epidemiological MSEIR Model Described by the Caputo Fractional Derivative," *International Journal of Dynamics and Control* 7 (2019): 776–784.

44. Z. M. Odibat and N. T. Shawagfeh, "Generalized Taylor's Formula," *Applied Mathematics and Computation* 186, no. 1 (2007): 286–293.

45. H.-L. Li, L. Zhang, H. Cheng, Y.-L. Jiang, and Z. Teng, "Dynamical Analysis of a Fractional-Order Predator-Prey Model Incorporating a Prey Refuge," *Journal of Applied Mathematics and Computing* 54 (2017): 435–449.

46. K. Diethelm and N. J. Ford, "Analysis of Fractional Differential Equations," *Journal of Mathematical Analysis and Applications* 265, no. 2 (2002): 229–248.

47. P. Van den Driessche and J. Watmough, "Reproduction Numbers and Sub-Threshold Endemic Equilibria for Compartmental Models of Disease Transmission," *Mathematical Biosciences* 180, no. 1–2 (2002): 29–48.

48. A. Jajarmi and D. Baleanu, "A New Fractional Analysis on the Interaction of HIV With CD4+ T-Cells," *Chaos, Solitons & Fractals* 113 (2018): 221–229.

49. B. Al-Hdaibat, M. A. Khan, I. Ahmad, E. Alzahrani, and A. Akgul, "Modeling and Analyzing the Dynamics of Brucellosis Disease With Vaccination in the Fractional Derivative Under Real Cases," *Journal of Applied Mathematics and Computing* 71 (2025): 1–22.

50. T.-C. Sun, M. H. DarAssi, W. F. Alfwzan, et al., "Mathematical Modeling of COVID-19 With Vaccination Using Fractional Derivative: A Case Study," *Fractal and Fractional* 7, no. 3 (2023): 234.

51. C. Li and F. Zeng, *Numerical Methods for Fractional Calculus* (CRC Press, 2015).

52. A. Malek and A. Hoque, "Mathematical Modeling of the Infectious Spread and Outbreak Dynamics of Avian Influenza With Seasonality Transmission for Chicken Farms," *Comparative Immunology, Microbiology and Infectious Diseases* 104 (2024): 102108.

53. E. A. Govorkova, T. Baranovich, P. Seiler, et al., "Antiviral Resistance Among Highly Pathogenic Influenza A (H5N1) Viruses Isolated Worldwide in 2002–2012 Shows Need for Continued Monitoring," *Antiviral Research* 98, no. 2 (2013): 297–304.

54. J.-H. Kwon, M. F. Criado, L. Killmaster, et al., "Efficacy of Two Vaccines Against Recent Emergent Antigenic Variants of Clade 2.3.2.1a Highly Pathogenic Avian Influenza Viruses in Bangladesh," *Vaccine* 39 (2021): 2824–2832.

55. M. S. Rahman, M. G. Rabbani, M. J. Uddin, A. Chakrabartty, and M. Naher, "Prevalence of Avian Influenza and Newcastle Disease Viruses Using Rapid Antigen Detection Kit in Poultry in Some Areas of Bangladesh," *Archives of Clinical Microbiology* 3, no. 1 (2012): 3.

56. L. F. Kanamori, M. Cox, G. J. Milinovich, R. J. S. Magalhaes, I. M. Mackay, and L. Yakob, "Heterogeneous and Dynamic Prevalence of Asymptomatic Influenza Virus Infections," *Emerging Infectious Diseases* 22 (2016): 1052–1056.

57. S. Payungporn, S. Chutinimitkul, A. Chaisingh, et al., "Discrimination Between Highly Pathogenic and Low Pathogenic H5 Avian Influenza A Viruses," *Emerging Infectious Diseases* 12 (2006): 700–701.

58. C. J. Galvin, A. Rumbos, J. I. Vincent, and M. Salvato, "Modeling the Effects of Avian Flu (H5N1) Vaccination Strategies on Poultry," *Codee Journal* 10 (2014): 1–10.

59. S. Yuan, "Drugs to Cure Avian Influenza Infection? Multiple Ways to Prevent Cell Death," *Cell Death & Disease* 4, no. 10 (2013): 835–e835.